

## Supporting Information

# Crystalline Transformations of Dinaphthyridinylamine Derivatives with Alteration of Solid-state Emission in Response to External Stimuli

Ryusuke Hagihara,<sup>1</sup> Naomi Harada,<sup>1</sup> Satoru Karasawa\*,<sup>1,2</sup> and Noboru Koga\*<sup>1</sup>

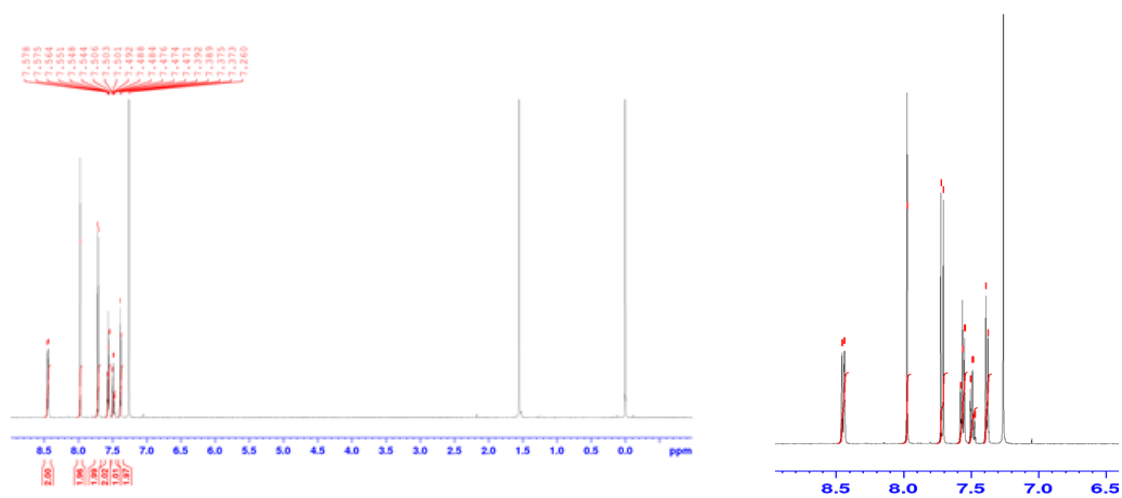
<sup>1</sup>. Graduate School of Pharmaceutical Sciences, Kyushu University, 3-1-1 Maidashi, Higashi-ku, Fukuoka, 812-8582 Japan

<sup>2</sup>. PRESTO, Japan Science and Technology Agency, Kawaguchi, 332-0012 Japan

### Contents

- S1. Figure S1. <sup>1</sup>H NMR spectra for **3-β** and **3-β'**.
- S2. Figure S2. Molecular structures and packings of **1** and water molecules forming 2-fold helical structure.
- S3. Figure S3. Molecular packing of **3-β'**.
- S4. Figure S4. Fingerprint plots by Harshfeld surface calculations of **3-α** and **3-β**.
- S5. Table S1. Photophysical properties of **1**, **2**, and **3** in various solvents.
- S6. Figure S5. Absorption and emission spectra of **1**, **2**, and **3** in various solvents.
- S7. Figure S6. Spectra of absorption for **1** - **3** and Emission for **1** and **2** in solid state. Emission spectra of the glass sample for **3**.
- S8. Figure S7. Emission spectra (a) and XRD patterns (b) of **3-α**, the ground powder of **3-α**, and the ground powder left under MeOH vapor
- S9. Figure S8. XRD patterns of **1** and **2**.
- S10. Figure S9. DSC profiles **1** and **2**.
- S11. Figure S10. DSC profile of the powder sample obtained from **3-α**.
- S12. Figure S11. XRD pattern of **3-β'**, the powder sample obtained from **3-β'** by grinding, and the resulting powder by heating at 100 °C together with the simulation obtained from the result of **3-α** by SXRD.
- S13. Figure S12. Photographs taken under irradiation at 365 nm for thermal transformation from powder (amorphous) to **3-α** and from **3-β'** to **3-α**.
- S14. Figure S13. Emission spectra of **3-β**, **3-β'**, and **3-β'** left under MeOH vapor for 1 day.

(a)



(b)

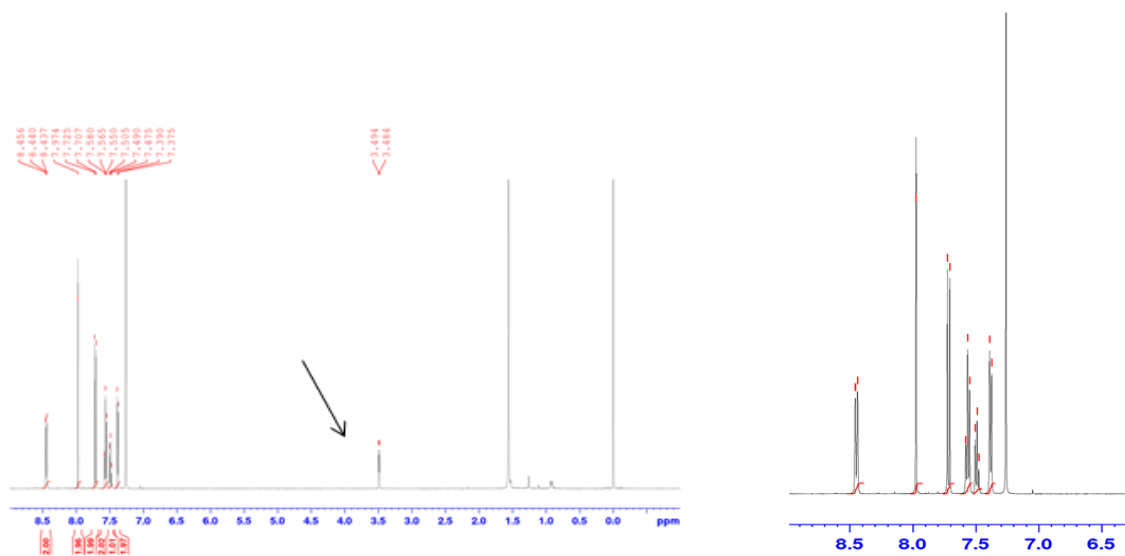
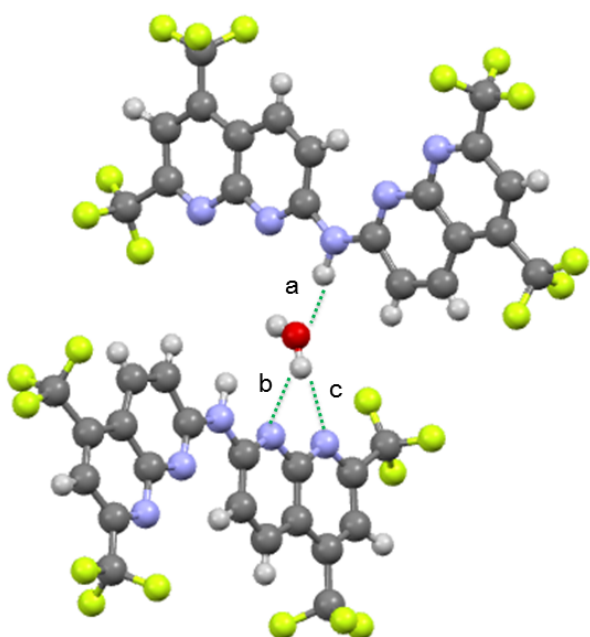


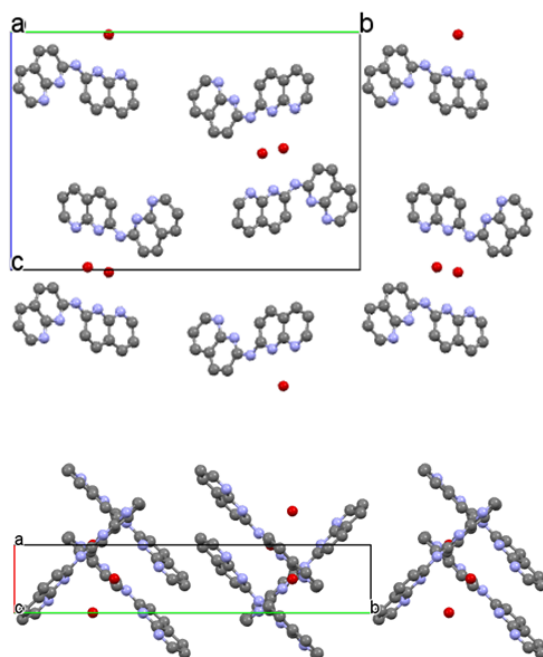
Figure S1.  $^1\text{H}$  NMR spectra of the crystals for **3- $\alpha$**  (a) and **3- $\beta$**  (b) dissolved in  $\text{CDCl}_3$ . Arrow in (b) indicates methyl group of MeOH molecules. Right figures are the expansion in the aromatic region.

S2.

(a)



(b)



(c)

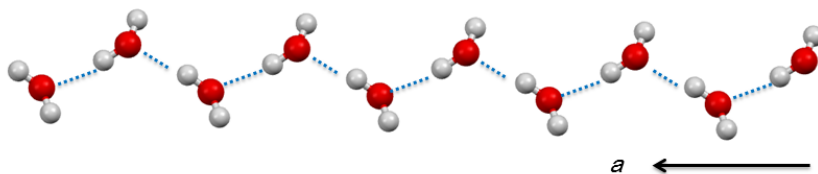
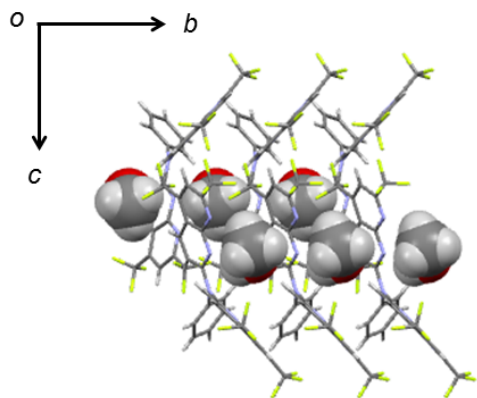
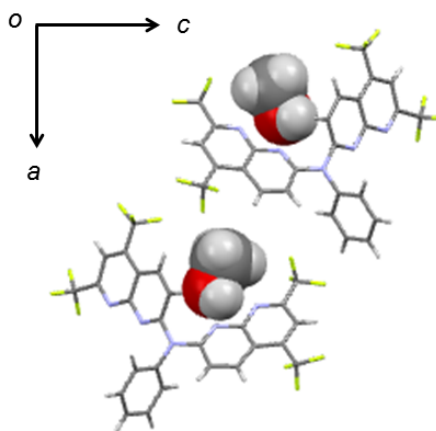


Figure S2. Molecular structures (a) and packings (b) of **1** and water molecules forming 2-fold helical structure (c). Green dotted line in (a) indicate hydrogen bonds between N atoms and a water molecule by 1.80 Å (a;  $r_{\text{H-O(H}_2\text{O)}}$ ), 2.495 Å (b;  $r_{\text{N-H(H}_2\text{O)}}$ ), and 2.135 Å (c;  $r_{\text{N-H(H}_2\text{O)}}$ ), respectively. Top and bottom in (b) represent views projecting along *a* and *c* axes, respectively and trifluoromethyl groups and H atoms are omitted for a sake of clarity. Sky blue dotted lines in (c) indicate hydrogen bonds by 2.034 Å within helical 1D structure of water molecules.

(a)



(b)



(c)

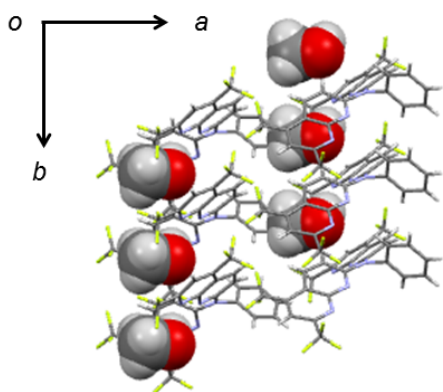
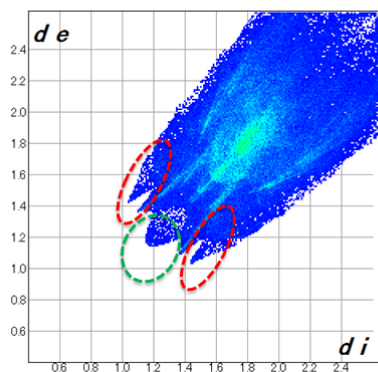


Figure S3. Molecular packing of  $3-\beta'$  projection of  $a$  (a),  $b$  (b), and  $c$  (c) axes, respectively. MeOH molecules are shown as space filling model.

S4.

(a)



(b)

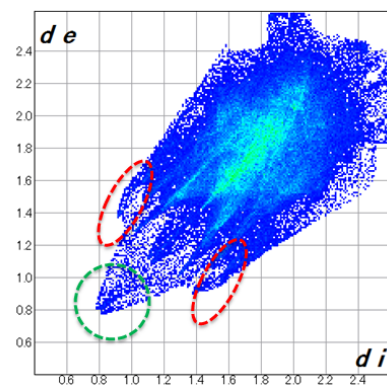


Figure S4. Fingerprint plots by Harshfeld surface calculations of **3-α** (a) and **3-β** (b). The red and green circles indicate the intermolecular short contact of CH-N and H-H, respectively.

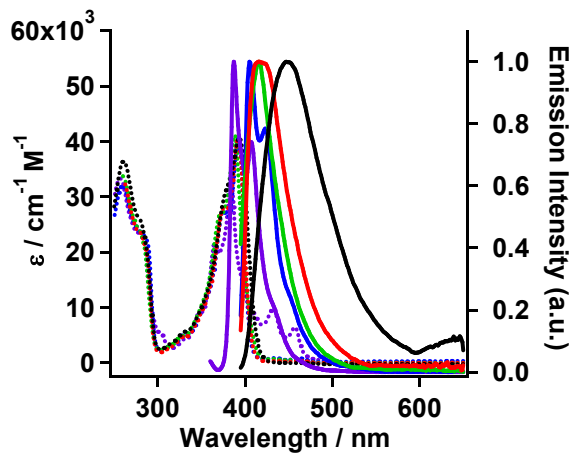
S5.

Table S1. Photophysical properties of **1**, **2**, and **3** in various solvents.

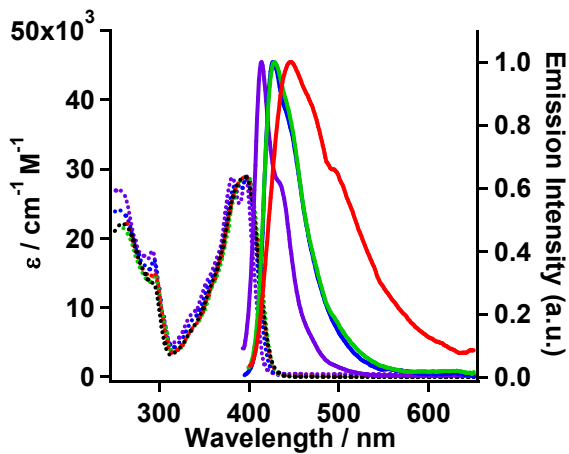
	<i>n</i> -hexane	Bu <sub>2</sub> O	CHCl <sub>3</sub>	AcOEt	MeOH
$\lambda_{\max}^{\text{abs}} / \text{nm} (\log \epsilon / \text{cm}^{-1} \text{M}^{-1})$					
<b>1</b>	384 (4.53)	392 (4.61)	388 (4.61)	392 (4.61)	393 (4.61)
<b>2</b>	396 (4.46)	398 (4.46)	399 (4.46)	396 (4.46)	395 (4.46)
<b>3</b>	390 (4.43)	390 (4.40)	393 (4.40)	391 (4.40)	392 (4.41)
$\lambda_{\max}^{\text{f}} / \text{nm} (\phi)$					
<b>1</b>	387 (0.09)	405 (0.26)	416 (0.21)	416 (0.38)	447 (0.09)
<b>2</b>	414 (0.08)	427 (0.12)	428 (0.25)	446 (0.17)	440 (0.01)
<b>3</b>	510 (0.25)	545 (0.08)	558 (0.04)	- (0.01 >)	- (0.01 >)
$\Delta^{\text{f-ab}} / \text{nm} (\text{cm}^{-1})$					
<b>1</b>	3 (3.3 x 10 <sup>6</sup> )	13 (7.7 x 10 <sup>5</sup> )	28 (3.6 x 10 <sup>5</sup> )	24 (4.2 x 10 <sup>5</sup> )	54 (1.9 x 10 <sup>5</sup> )
<b>2</b>	18 (5.6 x 10 <sup>5</sup> )	29 (3.4 x 10 <sup>5</sup> )	29 (3.4 x 10 <sup>5</sup> )	50 (2.0 x 10 <sup>5</sup> )	45 (2.2 x 10 <sup>5</sup> )
<b>3</b>	120 (8.3 x 10 <sup>4</sup> )	155 (6.5 x 10 <sup>4</sup> )	165 (6.1 x 10 <sup>4</sup> )	-	-

S6.

(a)



(b)



(c)

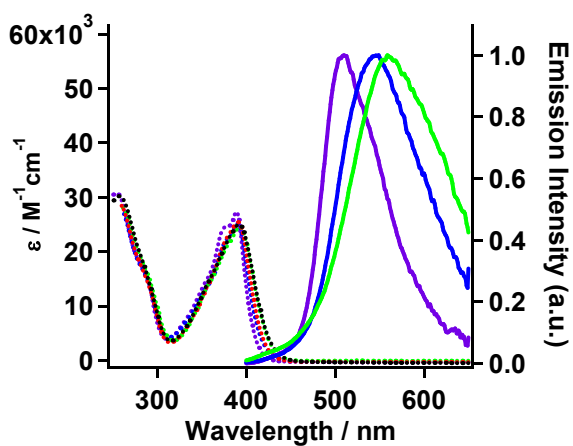
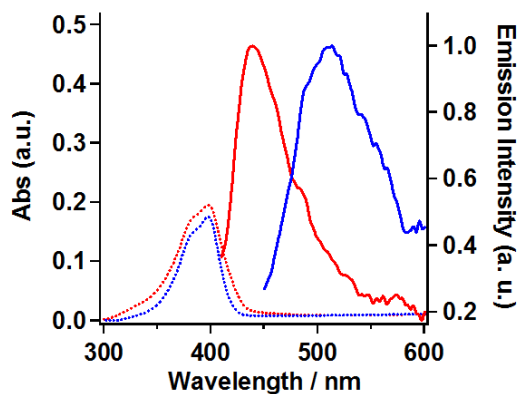
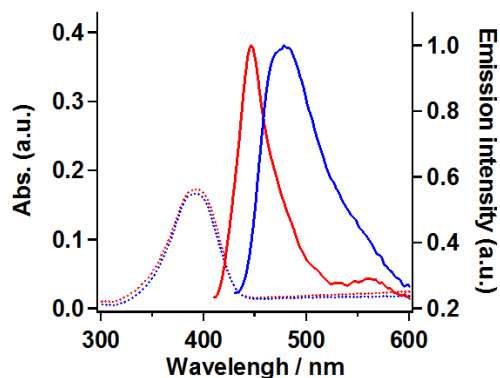


Figure S5. Absorption (dotted line) and emission (solid line) spectra of **1** (a), **2** (b), and **3** (c) in *n*-hexane (violet), Bu<sub>2</sub>O (blue), CHCl<sub>3</sub> (green), AcOEt (black), and MeOH (red), respectively.

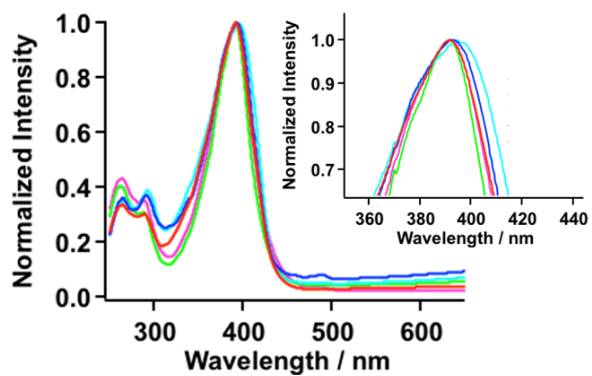
S7. (a)



(b)



(c)



(d)

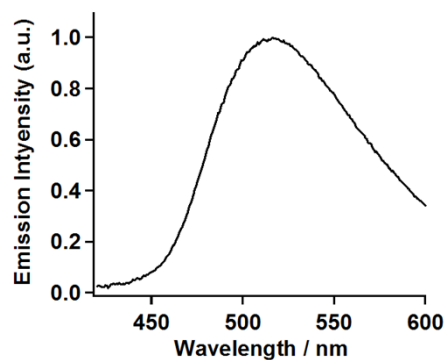


Figure S6. Absorption (dotted lines) and emission (solid lines) spectra of **1** (a) and **2** (b) in crystalline (red) and ground powder sample (blue). (c) Absorption spectra of **3** in **3- $\alpha$**  (light blue), **3- $\beta$**  (red), **3- $\beta'$**  (blue), glass (purple), and ground powder sample (green). Emission spectra of the glass sample for **3** (d).

S8.

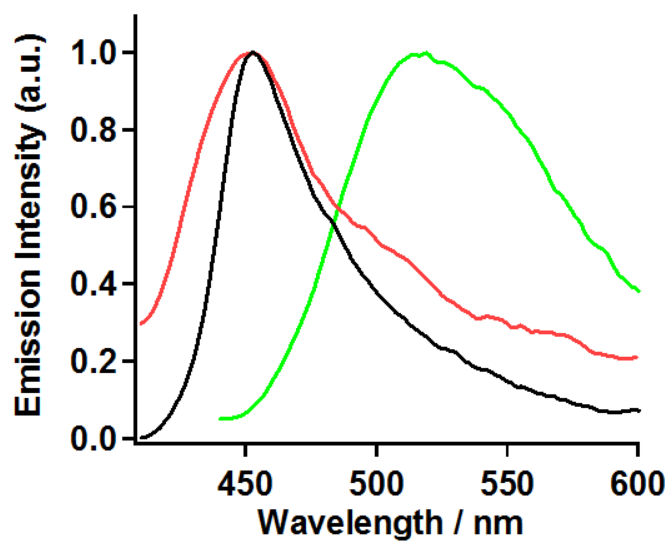


Figure S7a. Emission spectra of 3- $\alpha$  (black), the ground powder of 3- $\alpha$  (light green), and the ground powder left under MeOH vapor for 2 day (red).

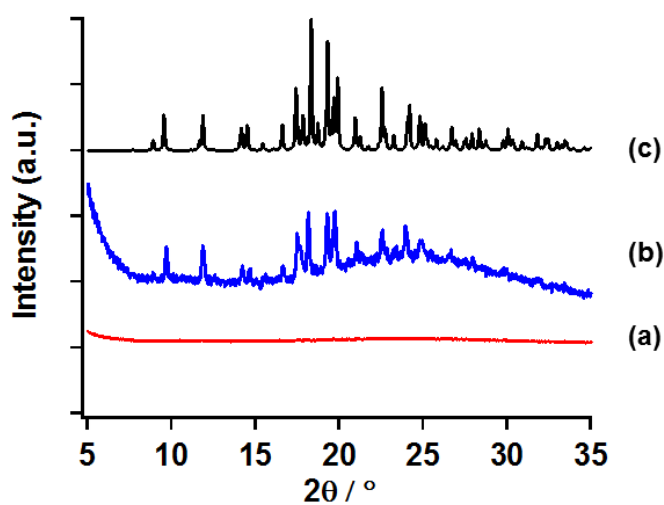
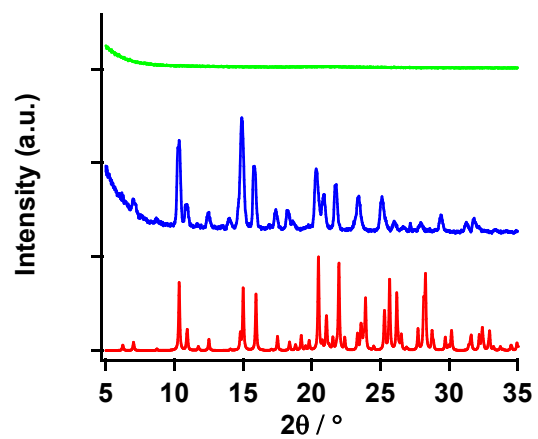


Figure S7b. Alteration of XRD patterns of the ground sample (red) of 3- $\alpha$ , subsequently exposed to MeOH vapor for 5 day (blue), and the simulation pattern (black) of 3- $\alpha$  obtained by SXRD.

S9.

(a)



(b)

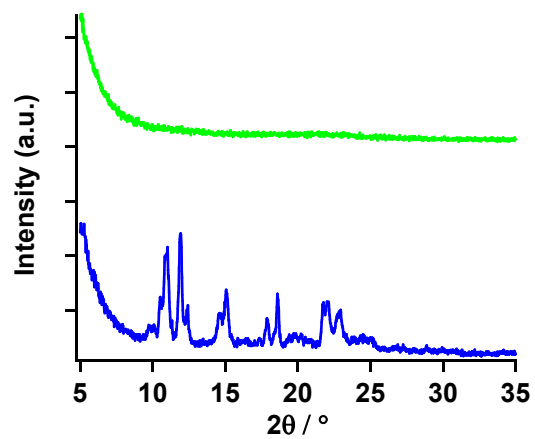


Figure S8. XRD patterns of the crystal (blue) and its ground samples (light green) for **1** (a) and **2**(b) with the simulation pattern (red).

S10.

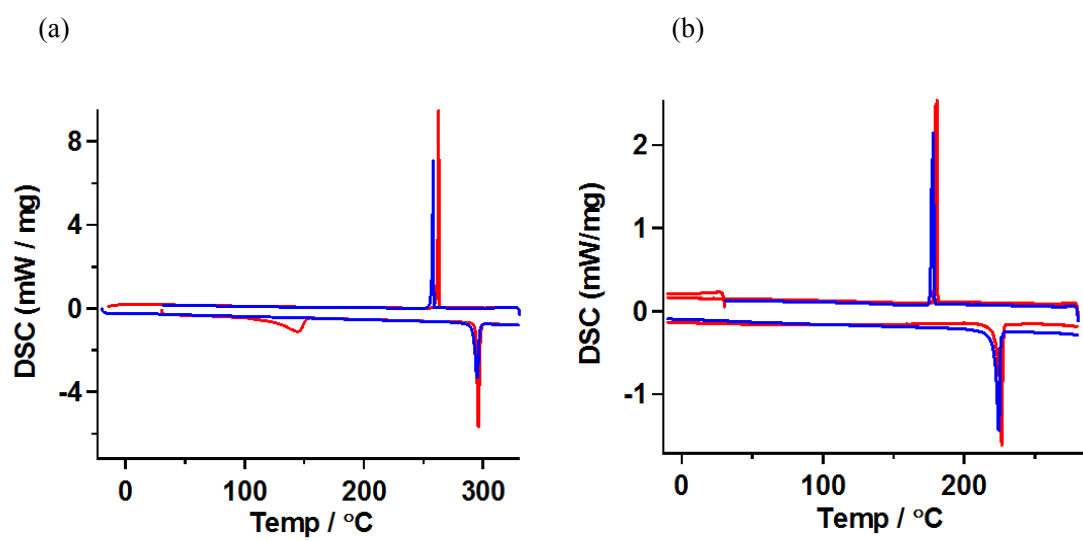


Figure S9. DSC profiles in the first (red line) and second (blue line) cycle of **1** (a) and **2**(b).

S11.

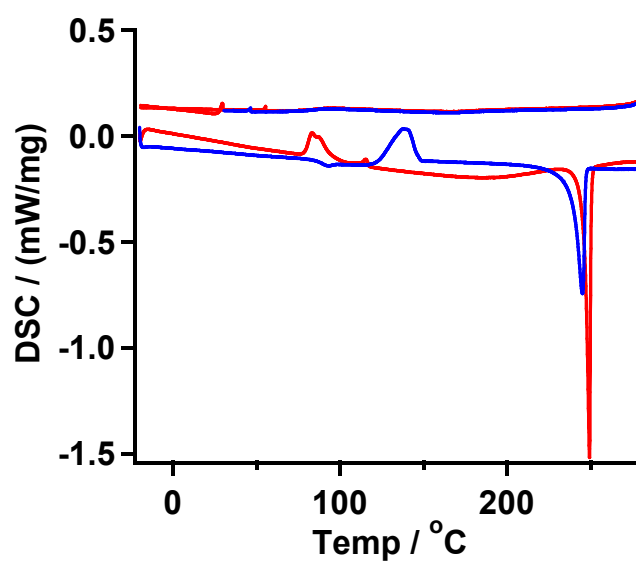


Figure S10. DSC profile of the powder sample obtained from  $3-\beta'$  by grinding in first (red) and second (blue) cycle.

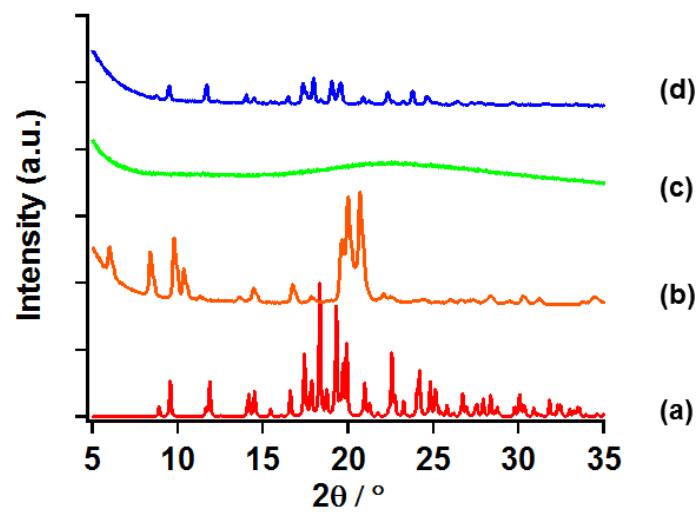
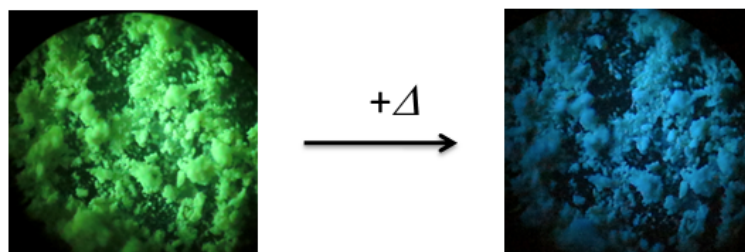


Figure S11. XRD pattern of  $3\text{-}\beta'$  (b), the powder obtained from  $3\text{-}\beta'$  by grinding (c), and the resulting powder by heating at  $100^\circ\text{C}$  together with the simulation obtained from the result of  $3\text{-}\alpha$  by SXR (a).

S13.

(a)



(b)

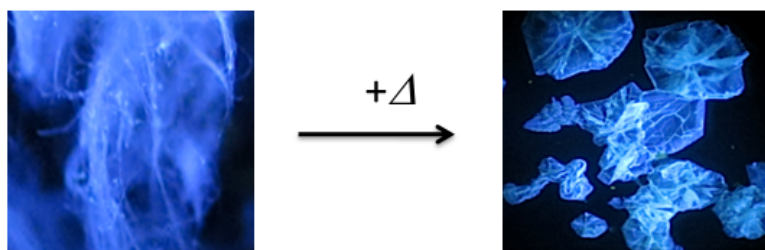


Figure S12. Photographs taken under irradiation at 365 nm for thermal transformation (a) from powders (amorphous) (left) to  $3-\alpha$  (right) and (b) from  $3-\beta'$  (left) to  $3-\alpha$  (right).

S14.

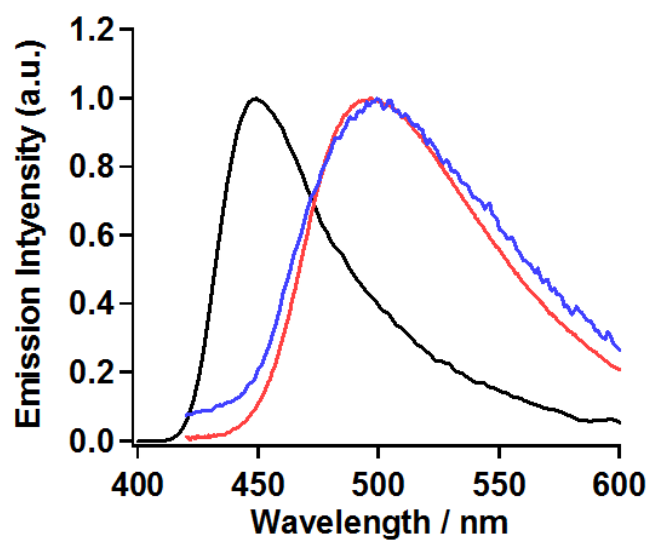


Figure S13. Emission spectra of 3- $\beta$  (red), 3- $\beta'$  (black), and 3- $\beta'$  left under MeOH vapor for 1 day (blue)